



# Numerical simulation of advection–diffusion equation with caputo-fabrizio time fractional derivative in cylindrical domains: Applications of pseudo-spectral collocation method

Qammar Rubbab<sup>a</sup>, Mubbashar Nazeer<sup>b</sup>, Fayyaz Ahmad<sup>c</sup>, Yu-Ming Chu<sup>d,e,\*</sup>,  
M. Ijaz Khan<sup>f,\*</sup>, Seifedine Kadry<sup>g</sup>

<sup>a</sup> Department of Mathematics, The Women University, Multan, Pakistan

<sup>b</sup> Department of Mathematics, Institute of Arts and Sciences, Government College University, Faisalabad, Chiniot Campus 35400, Pakistan

<sup>c</sup> Department of Applied Sciences, National Textile University Faisalabad 38000, Pakistan

<sup>d</sup> Department of Mathematics, Huzhou University, Huzhou 313000, PR China

<sup>e</sup> Hunan Provincial Key Laboratory of Mathematical Modeling and Analysis in Engineering, Changsha University of Science & Technology, Changsha 410114, PR China

<sup>f</sup> Department of Mathematics and Statistics, Riphah International University I-14, Islamabad 44000, Pakistan

<sup>g</sup> Department of Mathematics and Computer Science, Beirut Arab University, Beirut, Lebanon

Received 3 October 2020; revised 5 November 2020; accepted 14 November 2020

Available online 28 November 2020

## KEYWORDS

CF (Caputo-Fabrizio) fractional derivative;  
Advection-diffusion equation (ADE);  
Cylindrical coordinates;  
Integral transform, memory effects

**Abstract** The study of the unsteady fractional advection–diffusion equation (ADE) is carried out in cylindrical geometry along with time-exponential concentration on a cylindrical surface. We have used the Caputo-Fabrizio time-fractional derivative for the fractional model of the advection–diffusion. The analytical solutions for the solute concentration are determined by using integral transformations. For comparison, we also present a numerical scheme to get a numerical solution for different parameters' values. For time ordinary derivative approximation, we use the finite difference method. For space derivatives, we use a pseudo-spectral collocation method for higher-order accuracies. The advection-diffusion' classical model is obtained by taking the fractional parameter to be unit. The influence of the memory, namely, the Caputo-Fabrizio time-fractional derivative on the solute concentration is studied and compared with the ordinary case. Also, the impact of the drift velocity is analyzed by employing the Peclet number. It has been found that the concentration is decreasing with the Peclet number and is increasing with the radial coordinate. The present investigation will be helpful in future research to use a higher-order approximation for

\* Corresponding authors at: Department of Mathematics, Huzhou University, Huzhou 313000, PR China (Y.-M. Chu).  
E-mail addresses: [chuyuming@zjhu.edu.cn](mailto:chuyuming@zjhu.edu.cn) (Y.-M. Chu), [mikhan@math.qau.edu.pk](mailto:mikhan@math.qau.edu.pk) (M. Ijaz Khan).

Peer review under responsibility of Faculty of Engineering, Alexandria University.

<https://doi.org/10.1016/j.aej.2020.11.022>

1110-0168 © 2020 The Authors. Published by Elsevier B.V. on behalf of Faculty of Engineering, Alexandria University.  
This is an open access article under the CC BY license (<http://creativecommons.org/licenses/by/4.0/>).

ordinary derivatives. As the derivatives in space are ordinary derivatives, we use highly accurate pseudo-spectral collocation approximation for them.

© 2020 The Authors. Published by Elsevier B.V. on behalf of Faculty of Engineering, Alexandria University. This is an open access article under the CC BY license (<http://creativecommons.org/licenses/by/4.0/>).

## 1. Introduction

In various areas of physics, biology, and engineering, fractional calculus has achieved a milestone in applications of the areas as mentioned earlier [1–5]. The diffusion or heat conduction, along with the velocity field, transport process, or ground hydrology, is well explained by the time-fractional (ADE) advection–diffusion equation. This equation can be obtained as a result of the balanced equation for the time-nonlocal constitutive equation. Some problems modeled by the advection–diffusion are transport phenomena in food processing, groundwater solute transport, atmospheric pollutant transport, wellbores flows, porous soil solute diffusion, geothermal production with reinjection, and energy storage in porous media. The classical differential equation did not describe well many diffusion phenomena like super diffusion and slow diffusion. The time-fractional derivatives models describe such processes and their physical aspects very efficiently. Povstenko [6] has provided an excellent comparison of the sub-diffusion regime and the super-diffusion regime with ordinary diffusion. Various solution methods have been used to solve the (ADE) advection–diffusion equation due to its extensive application in different fields. Analytical solution to fractional (ADE) advection–diffusion equation with time-fractional pulses on the boundary has been found by Rubbab et al. [7]. A time-fractional heat conduction's solution with physical Robin condition on the sphere surface in a two-layered slab, and the perfect contact of layers has been presented by Kukla et al. [8]. Massabo et al. [9] have discussed the analytical solution by comparing it with the famous two-dimensional infinite domain with some limiting analytical solutions. Peclet numbers have been used to examine the influence of the boundary conditions on solutions, and the solution is compared with experimental data. The generalized analytical solution for ADE (advection–diffusion equation) in the finite space domain having an arbitrary time-dependent inlet boundary condition has been derived by Chen et al. [10]. An analytical solution of the convective-diffusion in two dimensions in a single fiber isotropic capillary membrane for solute transportation has been presented by Godongwana et al. [11].

Another essential analytical solution for the convection–diffusion problem has been discussed by Ivanchenko et al. [12]. The use of local fractional Laplace equation in solving fractional nonlinear CDE's (convection–diffusion equations) with improved Riemann-Liouville derivative has been studied by Merdan et al. [13]. The discretization method based on unstructured grids using a finite volume approach is proposed to solve CDE's (convection–diffusion equations) in r-z coordinates. A perfect control volume calculation method is presented by Yu et al. [14].

In this paper, the time-fractional differential equation is used for the advection–diffusion process in cylindrical geometry. Caputo and Fabrizio's time-fractional derivative is intro-

duced in formulating the governing equation. A new analytical solution of the ADE (advection–diffusion equation) in a cylindrical coordinate with initial and time-exponential boundary source is obtained by employing the integral transforms. The ordinary ADE (advection–diffusion equation) solution is a particular case of our solution by taking the limiting value of the fractional parameter of the time-derivative to be unit. The numerical calculations and graphical illustrations are used to present the fractional parameter (the memory effect, i.e., the effects on the flow with history) and the drift velocity ( $Pe$ , the Peclet number) on the concentration. To find the solution to a complex problem, the finite element method [15–21] and the finite difference method are famous. Numerical schemes are used to solve general-purpose problems. When we have to deal with fraction-order derivatives, the classical approach is not applicable for the discretization of fractional-order derivatives. The reason is apparent due to the global effect of fractional-order derivatives. Usually, fractional-order derivatives are presented in integrals, and ordinary derivatives are inside of them. In a numerical strategy, we first approximate the integral that gives us a linear combination of ordinary derivatives. Once we have an expression that involves ordinary derivatives, we may use a classical method to approximate ordinary derivatives. In the present research, we use the first-order approximation of ordinary derivatives using the forward difference method. It is of interest in future research to use a higher-order approximation for ordinary derivatives. As the derivatives in space are ordinary derivatives, we use highly accurate pseudo-spectral collocation approximation for them.

The paper is organized in the following manner. Section 1 has added the introduction based on the essential investigations on fractional derivative and numerical techniques. The scope of this investigation is also part of this section. Section 2 contains the mathematical formulation and analytical solution of the developed mathematical model. A brief introduction of the numerical technique, namely, the pseudo-spectral collocation method, is added in Section 3. A comparison between analytical and numerical solution is added in Section 4. The results and discussion of the numerical solution are highlighted in Section 5. This study's conclusions are added in the second last section, and the essential references related to this work are cited in the previous section of this paper.

## 2. Formulation of the problem and solution

The one-dimensional unsteady advection–diffusion equation with constant diffusivity  $D > 0$ , in the cylindrical domain with radius  $> 0$ , is given as, [12,14]

$$\frac{\partial \psi'(r', t')}{\partial t'} + \frac{V_0}{r'} \frac{\partial \psi'(r', t')}{\partial r'} = D \frac{1}{r'} \frac{\partial}{\partial r'} \left( r' \frac{\partial \psi'(r', t')}{\partial r'} \right),$$

$$r' \in [0, R], \quad t' \geq 0, \quad (1)$$

where  $\psi'(r', t')$  represents the species concentration and  $V_0$  the constant transport parameter.

Along with the advection–diffusion Eq. (1), with following initial and boundary conditions:

$$\psi'(r', 0) = \psi_0 \left( \frac{r'}{R} \right)^{V_0/D}, \quad (2)$$

$$\psi'(0, t') = 0, \quad \psi'(R, t') = \psi_0 \exp(-k_0 t'), \quad k_0 \geq 0, \quad (3)$$

where  $\psi_0$  is the constant species concentration. Consider the following dimensionless quantities

$$r = \frac{r'}{R}, \quad t = \frac{Dt'}{R^2}, \quad \psi = \frac{\psi'}{\psi_0}, \quad Pe = \frac{V_0}{D}, \quad (4)$$

Eqs. (1)–(3) take the form

$$\frac{\partial \psi(r, t)}{\partial t} + Pe \frac{1}{r} \frac{\partial \psi(r, t)}{\partial r} = \frac{1}{r} \frac{\partial}{\partial r} \left( r \frac{\partial \psi(r, t)}{\partial r} \right), \quad r \in [0, 1], \quad t \geq 0, \quad (5)$$

$$\psi(r, 0) = F(r) = r^{Pe}, \quad (6)$$

$$\psi(0, t) = 0, \quad \psi(1, t) = \exp(-a_0 t), \quad a_0 = \frac{k_0 R^2}{D}. \quad (7)$$

In the above relations, the Peclet number, namely, the advective and diffusive transport ratio. We introduce the following transformation in Eqs. (5)–(7)

$$\psi(r, t) = r^p \vartheta(r, t), \quad p = Pe/2, \quad (8)$$

we get

$$\left( \frac{p^2}{r^2} + \frac{\partial}{\partial t} \right) \vartheta(r, t) = \frac{\partial^2 \vartheta(r, t)}{\partial r^2} + \frac{1}{r} \frac{\partial \vartheta(r, t)}{\partial r}, \quad (9)$$

$$\vartheta(r, 0) = r^{-p} F(r) = G(r) = r^p, \quad (10)$$

$$\vartheta(0, t) = 0, \quad \vartheta(1, t) = \exp(-a_0 t). \quad (11)$$

The fractional form of the unsteady advection–diffusion Eq. (9) with CF (Caputo-Fabrizio) time-fractional derivative operator  ${}^{CF}D_t^\alpha$  can be written as

$${}^{CF}D_t^\alpha \vartheta(r, t) = \frac{\partial^2 \vartheta(r, t)}{\partial r^2} + \frac{1}{r} \frac{\partial \vartheta(r, t)}{\partial r} - \frac{p^2}{r^2} \vartheta(r, t), \quad (12)$$

where the CF (Caputo-Fabrizio) time-fractional derivative operator  ${}^{CF}D_t^\alpha$  is given by [22–23]

$${}^{CF}D_t^\alpha \vartheta(r, t) = \frac{1}{1-\alpha} \int_0^t \frac{\partial \vartheta(r, \tau)}{\partial \tau} \exp\left(\frac{-\alpha(t-\tau)}{1-\alpha}\right) d\tau, \quad 0 < \alpha < 1. \quad (13)$$

with the properties [6,18,19]:

$$L\{ {}^{CF}D_t^\alpha \vartheta(r, t) \} = \frac{qL\{\vartheta(r, t)\} - \vartheta(r, 0)}{(1-\alpha)q + \alpha}, \quad (14)$$

$$\lim_{\alpha \rightarrow 1} {}^{CF}D_t^\alpha \vartheta(r, t) = \frac{\partial \vartheta(r, t)}{\partial t}, \quad (15)$$

where  $L\{\vartheta(r, t)\} = \bar{\vartheta}(r, q) = \int_0^\infty \vartheta(r, t) e^{-qt} dt$  is the Laplace transform of a function  $\vartheta(r, t)$ . Eq. (13) is known as the first-order time discretization of the updated developed

fractional-order derivative. The information related to this operator can be seen from these Refs. [24,25].

### 2.1. Analytical solution for the time-fractional advection–diffusion process

To find an analytical solution for the fractional diffusion Eq. (12) along with the initial and boundary conditions (10) and (11), we will use Laplace transformation coupled with the finite Hankel transform of order  $p$ .

Applying the Laplace transform to Eqs. (11) and (12), using Eqs. (10) and (14), we obtain the following transformed form:

$$\frac{bq}{q + \alpha b} \bar{\vartheta}(r, q) - \frac{b}{q + \alpha b} G(r) = \left( \frac{\partial^2}{\partial r^2} + \frac{1}{r} \frac{\partial}{\partial r} - \frac{p^2}{r^2} \right) \bar{\vartheta}(r, q), \quad (16)$$

$$\bar{\vartheta}(0, q) = 0, \quad \bar{\vartheta}(1, q) = \frac{1}{q + a_0}, \quad (17)$$

where  $b = \frac{1}{1-\alpha}$ ,  $0 < \alpha < 1$ .

Now, applying the finite Hankel transform [26] of order  $p$  to Eq. (16) and by using Bessel functions' properties, we have

$$\begin{aligned} \frac{bq}{q + \alpha b} \bar{\vartheta}_p(s_n, q) - \frac{b}{q + \alpha b} \frac{J_{p+1}(s_n)}{s_n} \\ = s_n J_{p+1}(s_n) \bar{\vartheta}(1, q) - s_n^2 \bar{\vartheta}_p(s_n, q), \end{aligned} \quad (18)$$

where  $s_n$ ,  $n = 1, 2, \dots$  are the +ve roots of the transcendental equation  $J_p(x) = 0$  and  $\bar{\vartheta}_p(s_n, q) = \int_0^1 \vartheta(r, q) r J_p(rs_n) dr$  the finite Hankel transform of the function  $\bar{\vartheta}(r, q)$ .

Using Eqs. (17) and (18) we obtain

$$\begin{aligned} \bar{\vartheta}_p(s_n, q) = \frac{s_n J_{p+1}(s_n)}{q + a_0} \frac{q + \alpha b}{(b + s_n^2)q + \alpha b s_n^2} \\ + \frac{b}{(b + s_n^2)q + \alpha b s_n^2} \frac{J_{p+1}(s_n)}{s_n}. \end{aligned} \quad (19)$$

Eq. (19) can be simplified as

$$\begin{aligned} \bar{\vartheta}_p(s_n, q) = \frac{J_{p+1}(s_n)}{s_n(q + a_0)} + \frac{a_0 b J_{p+1}(s_n)}{s_n[(\alpha b - a_0)s_n^2 - a_0 b](q + a_0)} - \\ \frac{\alpha b^2 s_n J_{p+1}(s_n)}{(b + s_n^2)[(\alpha b - a_0)s_n^2 - a_0 b]} \frac{1}{q + \frac{\alpha b s_n^2}{b + s_n^2}} + \frac{b}{(b + s_n^2)} \frac{J_{p+1}(s_n)}{s_n} \frac{1}{q + \frac{\alpha b s_n^2}{b + s_n^2}}. \end{aligned} \quad (20)$$

Firstly, by applying inverse Laplace transform, inverse Hankel transform, and by using the integral [18]  $\int_0^1 r^{p+1} J_p(rs_n) dr = \frac{J_{p+1}(s_n)}{s_n}$ , we have

$$\begin{aligned} \vartheta(r, t) = r^p e^{-a_0 t} + 2a_0 b e^{-a_0 t} \sum_{n=1}^{\infty} \frac{J_p(rs_n)}{s_n[(\alpha b - a_0)s_n^2 - a_0 b] J_{p+1}(s_n)} - \\ 2a_0 b \sum_{n=1}^{\infty} \frac{J_p(rs_n)}{s_n[(\alpha b - a_0)s_n^2 - a_0 b] J_{p+1}(s_n)} \exp\left(-\frac{\alpha b s_n^2 t}{b + s_n^2}\right). \end{aligned} \quad (21)$$

By using Eq. (8), we get the species concentration corresponding to the time-fractional advection–diffusion process, as

$$\psi(r, t) = r^p \vartheta(r, t), \quad (22)$$

where  $\vartheta(r, t)$  is given by Eq. (21).

2.2. Analytical solution for the ordinary advection–diffusion process ( $\alpha \rightarrow 1, b \rightarrow \infty$ )

To find the solutions corresponding to the ordinary advection–diffusion process, we apply the limits  $\alpha \rightarrow 1, b \rightarrow \infty$  in Eq. (21)

$$\vartheta_c(r, t) = r^p e^{-a_0 t} + 2a_0 \sum_{n=1}^{\infty} \frac{J_p(rs_n)}{s_n(s_n^2 - a_0)J_{p+1}(s_n)} [\exp(-a_0 t) - \exp(-s_n^2 t)]. \quad (23)$$

where  $\vartheta_c(r, t) = \lim_{\substack{\alpha \rightarrow 1, \\ b \rightarrow \infty}} \vartheta(r, t)$ . The corresponding species concentration is given by

$$\psi_c(r, t) = r^p \vartheta_c(r, t). \quad (24)$$

3. Numerical technique

The numerical discretization of fractional order derivatives is challenging compared to the discretization of ordinary derivatives. We define initial  $t_1 = 0$  and final time  $t_n$ . We take uniform step-size  $\Delta t$  and  $n_t$  the total number of  $t$  grid-points. The time partition can be written as

$$\{t_1, t_2, t_3, \dots, t_n\}$$

Caputo-Fabrizio time-fraction derivative operation can be written as

$$CFD_t^\alpha \vartheta(r, t_i) = \frac{1}{1 - \alpha} \int_{t_j}^{t_i} \exp\left(\frac{-\alpha(t_i - \tau)}{1 - \alpha}\right) \frac{\partial \vartheta(t_i, \tau)}{\partial \tau} d\tau. \quad (25)$$

The integral can be subdivided into small intervals as

$$CFD_t^\alpha \vartheta(r, t_i) = \frac{1}{1 - \alpha} \sum_{j=1}^{i-1} \int_{t_j}^{t_{j+1}} \exp\left(\frac{-\alpha(t_i - \tau)}{1 - \alpha}\right) \frac{\partial \vartheta(t_i, \tau)}{\partial \tau} d\tau. \quad (26)$$

We can approximate the integral

$$\int_{t_j}^{t_{j+1}} \exp\left(\frac{-\alpha(t_i - \tau)}{1 - \alpha}\right) \frac{\partial \vartheta(t_i, \tau)}{\partial \tau} d\tau \approx \frac{\partial \vartheta(r, \tau)}{\partial \tau} \Big|_{\tau=t_{j+\frac{1}{2}}} \int_{t_j}^{t_{j+1}} \exp\left(\frac{-\alpha(t_i - \tau)}{1 - \alpha}\right) d\tau. \quad (27)$$

Furthermore, we can compute the integral

$$\int_{t_j}^{t_{j+1}} \exp\left(\frac{-\alpha(t_i - \tau)}{1 - \alpha}\right) d\tau, \text{ analytical, and it has the value } \frac{1}{1 - \alpha} \int_{t_j}^{t_{j+1}} \exp\left(\frac{-\alpha(t_i - \tau)}{1 - \alpha}\right) d\tau = \frac{1}{\alpha} \left(1 - \exp\left(\frac{-\alpha(t_i - \tau)}{1 - \alpha}\right)\right) \exp\left(\frac{\alpha \Delta t}{1 - \alpha}(j + 1 - i)\right). \quad (28)$$

And

$$g(j + 1 - i, \Delta t, \alpha) = \exp\left(\frac{\alpha \Delta t}{1 - \alpha}(j + 1 - i)\right).$$

For  $i = n_t$  and  $j = 1, 2, \dots, n_t - 1$ , we have the vector

$$\mathbf{g} = [g(0), g(-1), g(-2), \dots, g(2 - n_t)]^T. \quad (29)$$

We can construct a matrix of size  $(n_t - 1) \times (n_t - 1)$  form of the vector  $\mathbf{g}$  as

$$A = \begin{bmatrix} g(0) & & & & & \\ g(-1) & g(0) & & & & \\ g(-2) & g(-1) & g(0) & & & \\ \vdots & \vdots & \vdots & \ddots & & \\ g(2 - n_t) & g(2 - n_t) & \dots & g(-1) & g(0) & \end{bmatrix} \quad (30)$$

Approximation of time-fraction derivative can be written as

$$\begin{bmatrix} {}^{CF}D_t^\alpha \vartheta(r, t_1) \\ {}^{CF}D_t^\alpha \vartheta(r, t_2) \\ \vdots \\ {}^{CF}D_t^\alpha \vartheta(r, t_n) \end{bmatrix} \approx \begin{bmatrix} g(0) & & & & \\ g(-1) & g(0) & & & \\ g(-2) & g(-1) & g(0) & & \\ \vdots & \vdots & \vdots & \ddots & \\ g(2 - n_t) & g(3 - n_t) & \dots & g(-1) & g(0) \end{bmatrix} \begin{bmatrix} \frac{\partial \vartheta(r, \tau)}{\partial \tau} \Big|_{\tau=t_{1+\frac{1}{2}}} \\ \frac{\partial \vartheta(r, \tau)}{\partial \tau} \Big|_{\tau=t_{2+\frac{1}{2}}} \\ \vdots \\ \frac{\partial \vartheta(r, \tau)}{\partial \tau} \Big|_{\tau=t_{n_t-1+\frac{1}{2}}} \end{bmatrix} \quad (31)$$

The approximation of vector

$$\begin{bmatrix} \frac{\partial \vartheta(r, \tau)}{\partial \tau} \Big|_{\tau=t_{1+\frac{1}{2}}} \\ \frac{\partial \vartheta(r, \tau)}{\partial \tau} \Big|_{\tau=t_{2+\frac{1}{2}}} \\ \vdots \\ \frac{\partial \vartheta(r, \tau)}{\partial \tau} \Big|_{\tau=t_{n_t-1+\frac{1}{2}}} \end{bmatrix}$$

is computed as

$$\begin{bmatrix} \frac{\partial \vartheta(r, \tau)}{\partial \tau} \Big|_{\tau=t_{1+\frac{1}{2}}} \\ \frac{\partial \vartheta(r, \tau)}{\partial \tau} \Big|_{\tau=t_{2+\frac{1}{2}}} \\ \vdots \\ \frac{\partial \vartheta(r, \tau)}{\partial \tau} \Big|_{\tau=t_{n_t-1+\frac{1}{2}}} \end{bmatrix} \approx \frac{1}{\Delta t} \begin{bmatrix} 1 & & & & \\ -1 & 1 & & & \\ & -1 & 1 & & \\ & & -1 & 1 & \\ & & & -1 & 1 \end{bmatrix} \begin{bmatrix} \vartheta_2(r) \\ \vartheta_3(r) \\ \vdots \\ \vartheta_{n_t}(r) \end{bmatrix} 23em - \frac{\vartheta_1(r)}{\Delta t} \begin{bmatrix} 1 \\ 0 \\ \vdots \\ 0 \end{bmatrix}, \quad (32)$$

where  $\theta_i(r) = \vartheta(t_i, r)$ . By using the above approximation and (31), we get

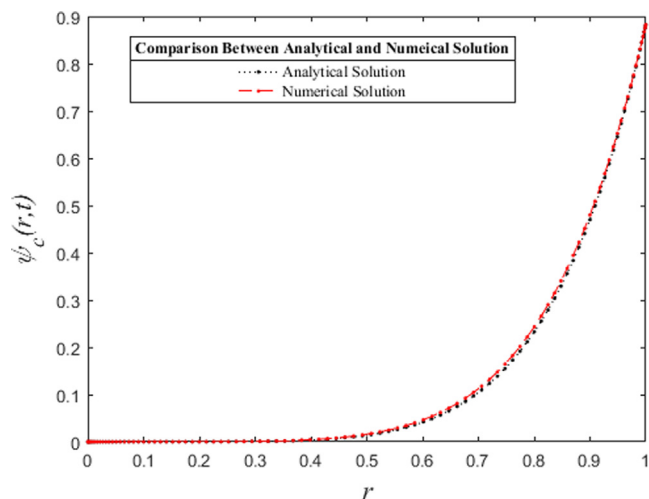
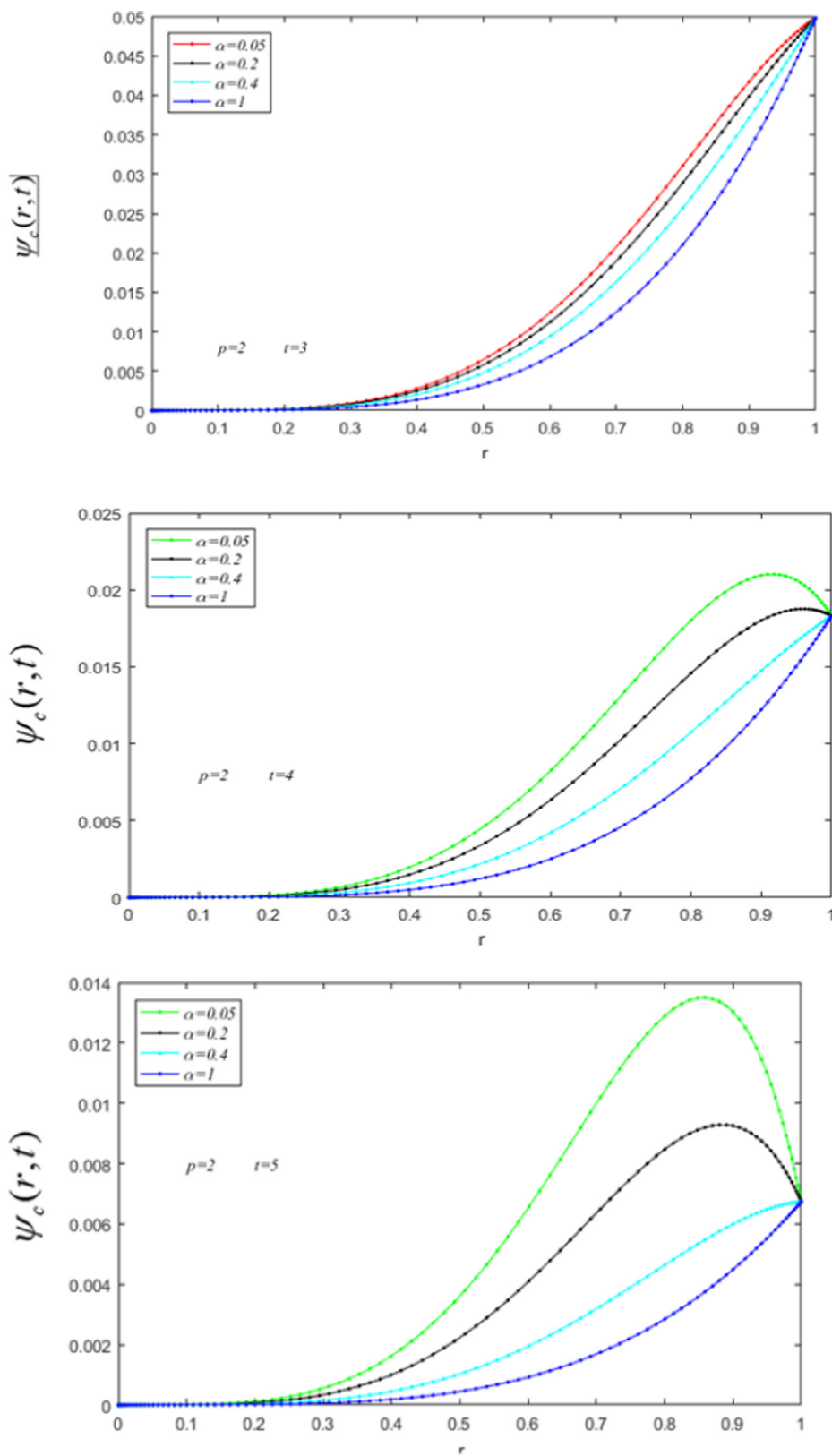
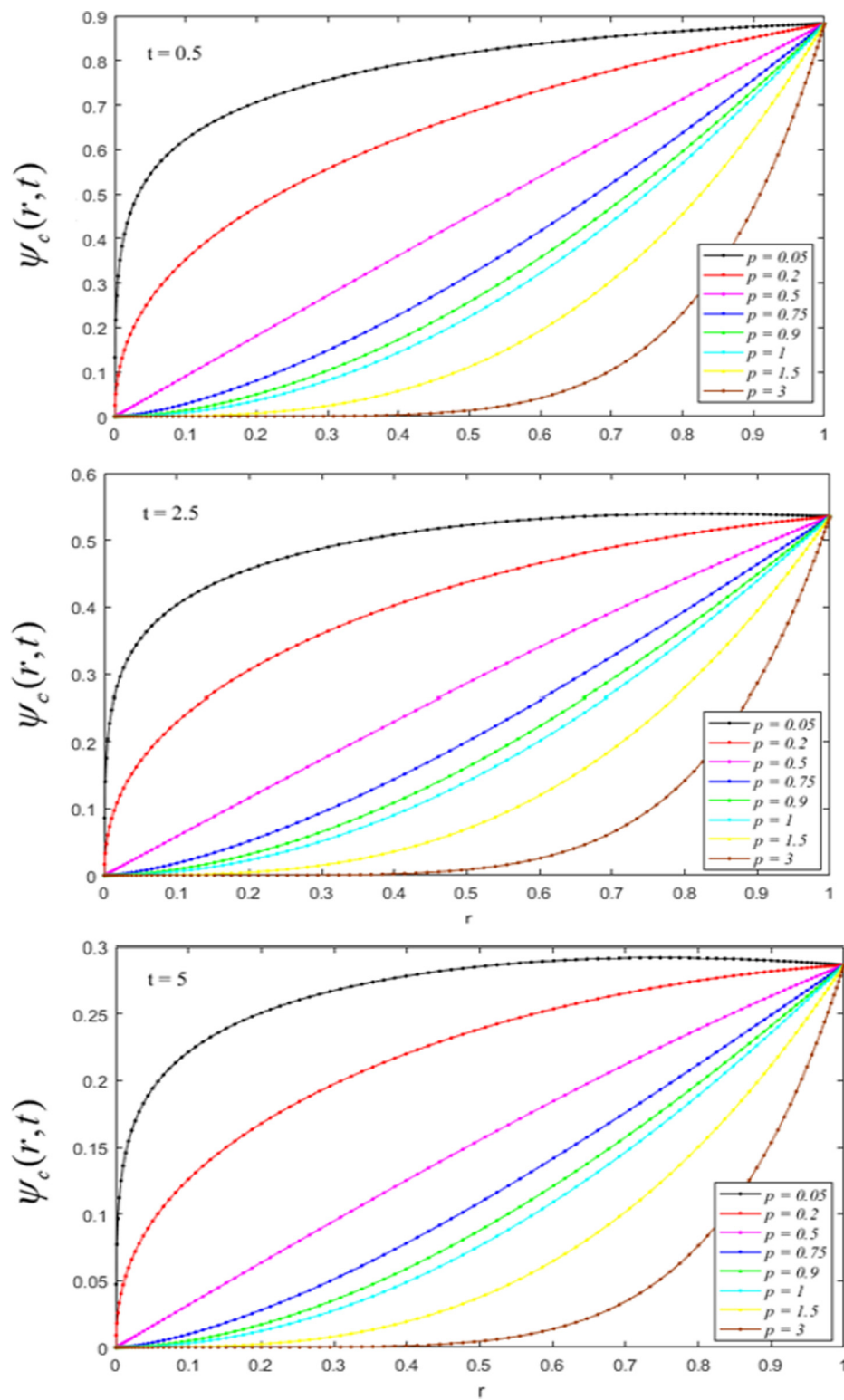


Fig. 1 Comparison between analytical and numerical solutions.



**Fig. 2** The dynamic evolution of the concentration  $\psi_c(r, t)$  for the different fractional parameters  $\alpha$  different values of the time  $t$ ,  $a_0 = 1$ , and Peclet number  $Pe = 4$ .



**Fig. 3** The dynamic evolution of the concentration  $\psi_c(r, t)$  for a range of the Peclet number, different time  $t$ ,  $a_0 = 0.25$ , and the fractional parameter  $\alpha = 0.5$ .

$$\begin{bmatrix} {}^{CF}D_t^\alpha \vartheta(r, t_1) \\ {}^{CF}D_t^\alpha \vartheta(r, t_2) \\ \vdots \\ {}^{CF}D_t^\alpha \vartheta(r, t_n) \end{bmatrix} \approx \frac{\eta}{\Delta t} AB\vartheta(r) \frac{\eta\vartheta_1(r)}{\Delta t} A \begin{bmatrix} 1 \\ 0 \\ \vdots \\ 0 \end{bmatrix}, \quad (33)$$

where

$$\vartheta(r) = \begin{bmatrix} \vartheta_2(r) \\ \vartheta_3(r) \\ \vdots \\ \vartheta_{n_r}(r) \end{bmatrix}$$

and

$$B = \begin{bmatrix} 1 & & & & \\ -1 & 1 & & & \\ & -1 & 1 & & \\ & & & -1 & 1 \end{bmatrix}$$

For space discretization, we use the pseudo-spectral collocation method. Let  $\mathbf{D}_1$  and  $\mathbf{D}_2$  are pseudo-spectral collocation operators for the approximation of first-order and second-order derivatives, respectively. We make the partition of  $r \in [0, 1]$  as  $\{r_1, r_2, \dots, r_{n_r}\}$ . The sizes of  $D_1$  and  $D_2$  are  $n_r$ . To deal with a second-order boundary value problem, we construct the following differential operator for our problem.

$$\mathbf{D} = \mathbf{D}_2(2 : n_r - 1, 2 : n_r - 1) + \text{diag}(1./\mathbf{r}(2 : n_r - 1)) \mathbf{D}_1(2 : n_r - 1, 2 : n_r - 1) - \text{diag}(p^2./\mathbf{r}(2 : n_r - 1)).^2, \quad (34)$$

where  $./$ , are the element-wise operation of division and power in Matlab format. The meaning of  $2 : n_r - 1$  is  $2, 3, \dots, n_r - 1$ . To accommodate the boundary conditions, we define two column vectors

$$\mathbf{d}_1 = \mathbf{D}_2(:, 1) + \text{diag}(1./\mathbf{r}(2 : n_r - 1))\mathbf{D}_1(:, 1) \quad (35)$$

$$\mathbf{d}_2 = \mathbf{D}_2(:, n_r) + \text{diag}(1./\mathbf{r}(2 : n_r - 1))\mathbf{D}_1(:, n_r),$$

where  $\mathbf{D}_{1or2}(:, i)$  means  $i$ th column of  $\mathbf{D}_{1or2}(:, i)$  matrix. We can write down the discretization of our problem in this form

$$\mathbf{M} = \mathbf{I} - \frac{\Delta t}{\eta} (\mathbf{D} \otimes \mathbf{C}),$$

$$\mathbf{m} = \frac{\Delta t}{\eta} (\mathbf{d}_1 \otimes \mathbf{C}\vartheta_1 + \mathbf{d}_2 \otimes \mathbf{C}\vartheta_{n_r} + \phi \otimes \mathbf{B}^{-1}\mathbf{e}_1), \quad (36)$$

where  $\mathbf{C} = (\mathbf{A}\mathbf{B})^{-1}$ ,  $\vartheta = [\vartheta_2, \vartheta_3, \dots, \vartheta_{n_r-1}]^T$ ,  $\vartheta_i = [\vartheta(r_i, t_2), \vartheta(r_i, t_3), \dots, \vartheta(r_i, t_{n_r})]^T$ ,  $\mathbf{e}_1$  is the first column identity matrix  $\mathbf{I}$ ,  $\vartheta_1$  and  $\vartheta_{n_r}$  are vectors for boundary conditions, and  $\phi$  is a vector that implements initial condition. The nonlinear equation is discretized by using a pseudo-spectral collocation method [26] based on Newton Raphson Method [27–30]. It is well-known that the pseudo-spectral collocation method offers high accuracy in the approximation of derivatives. To perform numerical simulation, we take the size of the system of nonlinear equation  $n = 100$ . The total number of equations is 200; we are solving a system of nonlinear coupled equations. In all the simulations, we take  $\mathbf{0}$  as an initial guess, and on average, we get numerical accuracy in the solution of a system of nonlinear equations.

Finally, by solving a system of linear equations

$$\mathbf{M}\vartheta = \mathbf{m},$$

we get the solution vector

$$\vartheta.$$

#### 4. Comparison between the analytical and numerical solution

For the validity of our analytical solution, which is obtained by the Laplace, transformation is compared with the numerical solution obtained with the help of the pseudo-spectral collocation method. The detail of this method is already mentioned in the previous section. We have constructed Fig. 1 to highlight the comparison of both solutions and noted that both solutions are very closed to each other.

#### 5. Numerical results and discussion

This section deals with the interpretation of the analytical results for the solute concentration with the graphical illustrations. We have used Mathcad software for numerical results. Fig. 2 illustrates the effects of the fractional parameter on the solute concentration  $\psi_c(r, t)$ . It has been seen that neat the surface of the cylinder there exists values of the fractional parameter  $\alpha$  for which the solute concentration with respect to the fractional advection–diffusion process is higher as compared with the ordinary model. Moreover, the converse behavior has been also observed for some other values of the fractional parameter  $\alpha$ . In conclusion, the fractional parameter  $\alpha$  which indicates the memory effects (i.e. the effects on the history of the flow) has a significant influence on the solute concentration as compared with the ordinary model of the advection–diffusion process. Fig. 3 describes the effects of  $Pe$  (Peclet number) on the concentration  $\psi_c(r, t)$ . It has been observed that drift velocity changes equivalent to the change in the Peclet number. The domination of the (diffusion or the advection) transport process is shown by the Peclet number. A decrease in solute concentration has been observed with the increase in Peclet number whereas the concentration increases with the radial coordinate  $r$ . For  $Pe = 1$  ( $p = 0.50$ ), the solute concentration  $\psi_c(r, t)$  increases almost linear.

#### 6. Conclusions

In the present research, we use the first-order approximation of ordinary derivatives by using the forward difference method. It is of interest in future research to use a higher-order approximation for ordinary derivatives. As the derivatives in space are ordinary derivatives, we use highly accurate pseudo-spectral collocation approximation for them.

#### Declaration of Competing Interest

The authors declare that they have no known competing financial interests or personal relationships that could have appeared to influence the work reported in this paper.

## References

- [1] W. Gao, H. Günerhan, H.M. Baskonus, Analytical and approximate solutions of an epidemic system of HIV/AIDS transmission, *Alex. Eng. J.* 59 (2020) 3197–3211.
- [2] Z. Sabir, D. Baleanu, M. Shoaib, M.A.Z. Raja, Design of stochastic numerical solver for the solution of singular three point second-order boundary value problems, *Neural Computing and Applications*, 10.1007/s00521-020-05143-8.
- [3] W. Gao, P. Veerasha, D.G. Prakasha, H.M. Baskonus, G. Yel, New approach for the model describing the deathly disease in pregnant women using Mittag-Leffler function, *Chaos Solitons Fract.* 134 (2020) 109696.
- [4] F. Mohammadi, L. Moradi, D. Baleanu, A. Jajarmi, A hybrid functions numerical scheme for fractional optimal control problems: Application to nonanalytic dynamic systems, *J. Vib. Control* 24 (21) (2018) 5030–5043.
- [5] S.S. Sajjadi, D. Baleanu, A. Jajarmi, H.M. Pirouz, A new adaptive synchronization and hyperchaos control of a biological snap oscillator, *Chaos Solitons Fract.* 138 (2020) 109919.
- [6] Y. Povstenko, *Linear Fractional Diffusion-wave Equation for Scientists and Engineers*, Springer International Publishing, Switzerland, 2015.
- [7] Q. Rubbab, I.A. Mirza, M.Z.A. Qureshi, Analytical solution to fractional advection-diffusion equation with time-fractional pulses on the boundary, *AIP Adv.* 6 (2016) 075318.
- [8] S. Kukla, U. Siedlecka, Laplace transform solution of the problem of time-fractional heat conduction in a two-layered slab, *J. Appl. Math. Comput. Mech.* 14 (4) (2015) 105–113.
- [9] M. Massabo, R. Cianci, O. Paladino, An analytical solution of the advection dispersion equation in a bounded domain and its applications to laboratory experiments, *J. Appl. Math.* (2011), <https://doi.org/10.1155/2011/493014>.
- [10] J.S. Chen, C.W. Liu, Generalized analytical solution for advection-dispersion equation in finite spatial domain with arbitrary time-dependent inlet boundary condition, *Hydrol. Earth Syst. Sci.* 15 (2011) 2471–2479, <https://doi.org/10.5194/hess-15-2471-2011>.
- [11] B. Godongwana, D. Solomons, M.S. Sheldon, A solution of the convective-diffusion equation for solute mass transfer inside a capillary membrane bioreactor, *Int. J. Chem. Eng.* 2010 (2010). Article ID 38482.
- [12] O. Ivanchenko, N. Sindhwani, A.A. Linninger, Exact solution of the Diffusion-Convection equation in cylindrical geometry, *AIChE J.* (2011), <https://doi.org/10.1002/aic.12663>.
- [13] M. Merdan, Analytical approximate solutions of fractional convection-diffusion equation by means of local fractional derivative operators, *Br. J. Math. Comput. Sci.* 16 (4) (2016) 1–15. Article no. BJMCS.25827.
- [14] G. Yu, B. Yu, Y. Zhao, J. Li, Q. Shao, J. Xie, An unstructured grids-based discretization method for convection–diffusion equations in the two-dimensional cylindrical coordinate systems, *Int. J. Heat and Mass Transfer* 67 (2013) 581–592.
- [15] Y.M. Chu, M.I. Khan, N.B. Khan, S. Kadry, S.U. Khan, I. Tlili, M.K. Nayak, Significance of activation energy, bio-convection and magnetohydrodynamic in flow of third grade fluid (non-Newtonian) towards stretched surface: A Buongiorno model analysis, *Int. Commu. Heat Mass Transf.* 118 (2020) 104893.
- [16] A. Shafiq, C.M. Khalique, Lie group analysis of upper convected Maxwell fluid flow along stretching surface, *Alex. Eng. J.* 59 (2020) 2533–2541.
- [17] M.Z. Ullah, T.S. Jang, An efficient numerical scheme for analyzing bioconvection in von-Kármán flow of third-grade nanofluid with motile microorganisms, *Alex. Eng. J.* 59 (2020) 2739–2752.
- [18] M. Nazeer, N. Ali, T. Javed, Numerical simulation of MHD flow of micropolar fluid inside a porous inclined cavity with uniform and non-uniform heated bottom wall, *Can. J. Phys.* 96 (6) (2018) 576–593.
- [19] N. Ali, M. Nazeer, T. Javed, Muhammad Arshad Siddiqui, Buoyancy driven cavity flow of a micropolar fluid with variably heated bottom wall, *Heat Trans. Res.* 49 (5) (2018).
- [20] N. Ali, F. Nazeer, M. Nazeer, Flow and heat transfer analysis of Eyring-powell fluid in a pipe, *Zeitschrift für Naturforschung A (ZNA)* 73 (3) (2018) 265–274.
- [21] M. Nazeer, N. Ali, T. Javed, Effects of moving wall on the flow of micropolar fluid inside a right angle triangular cavity, *Int. J. Numer. Meth. Heat Fluid Flow* 28 (10) (2018) 2404–2422.
- [22] A. Jajarmi, D. Baleanu, A new iterative method for the numerical solution of high-order non-linear fractional boundary value problems, *Front. Phys.* 20 (2020) 1–8.
- [23] D. Baleanu, B. Ghanbari, J.H. Asad, A. Jajarmi, H.M. Pirouz, Planar system-masses in an equilateral triangle: numerical study within fractional calculus, *Comput. Model. Eng. Sci.* 124(3), 953–968.
- [24] A.D. Poularikas, in: Alexander D. Poularikas (Ed.), *The Transforms and Applications Handbook*, second ed. CRC Press LLC, Boca Raton, 2000.
- [25] S. Qureshi, N.A. Rangaig, D. Baleanu, New numerical aspects of caputo-fabrizio fractional derivative operator, *Mathematics* 7 (4) (2019) 374.
- [26] M. Caputo, M. Fabrizio, A new definition of fractional derivative without singular kernel, *Progr. Fract. Differ. Appl.* 1 (92) (2015) 73–85.
- [27] M.I. Khan, M. Waqas, T. Hayat, A. Alsaedi, A comparative study of Casson fluid with homogeneous-heterogeneous reactions, *J. Colloid Interface Sci.* 498 (2017) 85–90.
- [28] R. Muhammad, M.I. Khan, M. Jameel, N.B. Khan, Fully developed Darcy-Forchheimer mixed convective flow over a curved surface with activation energy and entropy generation, *Comput. Methods Programs Biomed.* 188 (2020) 105298.
- [29] M.I. Khan, S. Qayyum, T. Hayat, A. Alsaedi, Entropy generation minimization and statistical declaration with probable error for skin friction coefficient and Nusselt number, *Chin. J. Phys.* 56 (4) (2018) 1525–1546.
- [30] S. Qayyum, M.I. Khan, T. Hayat, A. Alsaedi, Comparative investigation of five nanoparticles in flow of viscous fluid with Joule heating and slip due to rotating disk, *Physica B* 534 (2018) 173–183.